Quaternized zinc(II) phthalocyanine-sensitized TiO₂: surfactant-modified sol–gel synthesis, characterization and photocatalytic applications

İlknur Altın*, Münevver Sökmen, Zekeriya Bıyıklıoğlu

Faculty of Science, Department of Chemistry, Karadeniz Technical University, 61080 Trabzon, Turkey, Tel. +90 462 377 25 32; Fax: +90 462 325 31 96; emails: ilknurtatlidil@ktu.edu.tr (İ. Altın), msokmen@ktu.edu.tr (M. Sökmen), Tel. +90 462 377 36 74; Fax: +90 462 325 31 96; email: zekeriya_61@yahoo.com (Z. Bıyıklıoğlu)

ABSTRACT

TiO₂ nanoparticles and zinc phthalocyanine-sensitized TiO₂ (ZnPc/TiO₂) nanocomposite were synthesized in the presence and absence of Triton X100 (a nonionic surfactant) by a modified sol–gel method to improve the photocatalytic activity of TiO₂ under near visible light (365 nm). A novel quaternized ZnPc molecule was used as sensitizer. Prepared nanoparticles and nanocomposite were characterized by scanning electron microscopy, energy dispersive analysis, X-ray diffractometry, transmission electron microscopy (TEM), Brunauer–Emmett–Teller, thermogravimetry analysis, and UV–vis–NIR. The results demonstrated that the ZnPc was successfully loaded on the TiO₂ nanoparticles and the nanocomposite possesses the anatase crystalline phase with the specific surface area of 110.04 m² g⁻¹. The TEM micrograph showed that the average grain crystal size is 5–15 nm. ZnPc in the TiO₂ structure shifted the absorption edge to visible region. The photocatalytic activities of prepared photocatalysts (ZnPc/TiO₂, ZnPc/TiO₂-TX100, TiO₂, and TiO₂-TX100) were evaluated for degradative removal of methyl orange and reductive removal of Cr(VI) ions as test pollutants. Results of photocatalytic removal revealed that the ZnPc/TiO₂-TX100 has shown much more photocatalytic efficiencies than the ZnPc/TiO₂ prepared without TX100 and neat TiO₂ prepared with or without TX100. Therefore, this sol–gel method modified with TX100 is useful in the preparation of nanostructure ZnPc/TiO₂ with high photocatalytic activity and higher surface area.

Keywords: Zinc phthalocyanine; Sensitization; TiO₂; Photocatalytic activity; Surfactant

1. Introduction

Water is one of the most valuable and indispensable natural resources for health and quality of life on the earth, and it is under threat from various pollutants such as textile, metal plating, pesticides, and paper industries as a result of development of industrialization and rising of population. The providing of safe and clean water is one of the most important environment issues what humanity and aquatic organisms are facing in these days [1,2]. In recent years, many technologies have been developed to remove pollutants such as textile dyes and toxic metal ions present in wastewater before discharge. Water purification methods can be biological, physical, or chemical for destruction of effluents [3,4].

*Corresponding author.

Conventional wastewater treatment techniques can transfer the pollutants from one phase to another and causing secondary pollution; thus, they are not economical and effective [5,6]. Therefore, more economical and environment-friendly techniques need to be designed. In this context, semiconductor-based heterogeneous photocatalysis has attracted much attention to remove the contaminants both in aqueous and gaseous phase particularly when used under solar or artificial near visible light [7–9]. Among the various metal oxide semiconductors, TiO_2 is the most frequently used photocatalyst due to low cost, non-toxicity, and high stability [10–12]. Although, heterogeneous photocatalytic processes are not exactly understood, some approaches are already accepted and have been discussed detailed in the literature [13,14]. Briefly, when TiO_2 photocatalyst is irradiated with the proper UV light ($hv \geq$ its band gap), an electron may be transferred from the valence band (VB) to the conduction band (CB) leaving behind a positively charged hole. These charge carriers produce highly reactive oxygen species such as hydroxyl (·OH), superoxide (O_2^{-}), and hydroperoxy (HO_2^{-}) radicals, and they participate in redox reactions with species being catalyst surface [15,16]. These highly reactive agents play an important role in the photocatalytic oxidation of organic pollutants including synthetic dyes, while the photo-generated electrons are responsible for the photocatalytic reduction of toxic heavy metal ions. Toxic metal ions such as Cr(VI) ions can be reduced to non-toxic Cr(III) ions with photo-generated electrons [17]. Although TiO_2 has excellent photocatalytic properties compared to other photocatalyst, its photocatalytic activity is limited by tendency of electron–hole recombination and low absorption in visible region [18,19]. Many methods have been developed to enhance the photocatalytic efficiency of TiO_2, such as metal doping, non-metal doping, coupling of semiconductor systems, and organic dye sensitization of the photocatalyst [20–23]. Among these methods, dye photosensitization has gained attention due to its stability and improving the photocatalytic performance of the catalyst. In this approach, organometallic dyes such as phthalocyanine (Pc) (possess absorption in blue-green region) attached to the TiO_2 surface (Pc-TiO_2) facilitate the visible light absorption. As a result of light absorption, excited phthalocyanine molecule (Pc*) is produced. Singlet oxygen is also generated by the interaction of molecular oxygen and excited Pc*. Thereby, the excited species can inject electrons into the CB of TiO_2, followed by the generation of Pc cation radical (Pc·+) and superoxide anion radical (O_2^{-}) (Eq. (3)). Pc cation radical can oxidize organic

substrate (R) along with recovery of original phthalocyanine (Eqs. (1)–(5)) [24].

$$Pc + hv \rightarrow Pc^* \tag{1}$$

$$Pc^* + O_2 \rightarrow Pc + {}^1O_2 \tag{2}$$

$$Pc^* + TiO_2 \rightarrow Pc^{\cdot+} + TiO_2\left(e_{CB}^-\right) \tag{3}$$

$$TiO_2\left(e_{CB}^-\right) + O_2 \rightarrow TiO_2 + O_2^{\cdot-} \tag{4}$$

$$Pc^{\cdot+} + R \rightarrow Pc + R^{\cdot+} \tag{5}$$
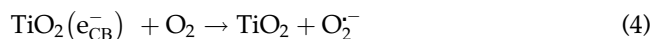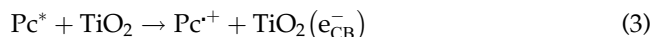
Presence of metal ion in Pc structure increases the electron transfer and intense absorption bands in the longer wavelength. A variety of methods such as sol–gel, spin coating, immersion, hydrothermal method, and so forth have been developed to prepare dye photosensitization of TiO_2 with phthalocyanines [25,26]. Sol–gel method has been preferred for improved photocatalytic activity since TiO_2 was commonly prepared at nano level and had large surface area. So, the usage of surfactant, which is especially bio-organic and non-toxic, is an advantage to improve photocatalytic efficiency of the catalyst [27,28]. This improvement is mainly related to decreased particle size and increased specific surface area. Surfactants play an important role to keep the nanoparticles apart from each other during the sol–gel process.

Metallo-phthalocyanine-TiO_2 nanocomposites (MPc/TiO_2) have been successfully used for degradation of phenols, methyl orange (MO), and sulfide. The composites have also been applied for the reduction of CO_2 and Cr(VI) [29,30]. Meanwhile, removal studies of the pollutants reveal that MPc/TiO_2 photocatalyst has exhibited good activity. Wu et al. [31] reported that Fe_3O_4@SiO_2@TiO_2@CoPcS hierarchical nanostructure showed excellent photocatalytic efficiency for the photocatalytic degradation of methylene blue under UV–vis and visible light. Guo et al. [32] reported that the H_2O_2-assisted one-dimensional 2,9,16,23-tetra-nitrophthalocyanine iron (II) (TNFePc)/TiO_2 nanofiber heterostructures possessed higher MO (10 mg L^{-1}) degradation (94%) than pure TiO_2 (11%) and TNFePc/TiO_2 nanofiber without H_2O_2 (48%) within 3 h light exposure. Wang et al. [33] report about improvement of carbon dioxide photocatalytic reduction efficiency under simulated solar radiation using zinc phthalocyanine-modified TiO_2 catalyst (ZnPc/TiO_2) prepared by microwave-hydrothermal methods. They found that CO_2 photocatalytic reduction was improved by microwave treatment (about four times higher).

In this study, we have synthesized a new TiO_2 photocatalyst containing quaternized zinc phthalocyanine ($ZnPc/TiO_2$) as photosensitizer using sol–gel method. Presence of surfactant in the sol is expected to play an important role for increased surface area and photocatalytic efficiency. Triton X100 (TX100), a nonionic surfactant, was used for the synthesis of nanoparticles since it could be easily removed from the reaction media during calcination. To the best of our knowledge, no study has been reported so far showing photocatalytic removal pollutants employing $ZnPc/TiO_2$ synthesized in the presence of TX100. The aim of the study was to investigate the structural properties and photocatalytic activity of the prepared materials for photocatalytic removal of the organic or inorganic model pollutants. Methyl orange (MO) and highly toxic Cr(VI) ions were chosen as model pollutants owing to their wide industrial applications. The morphology of prepared materials was characterized by scanning electron microscopy (SEM), energy dispersive analysis (EDX), transmission electron microscopy (TEM), X-ray diffractometry (XRD), UV–vis spectroscopy, and Brunauer–Emmett–Teller (BET), and thermogravimetry analysis (TGA).

2. Experimental

2.1. Synthesis of 1(4), 8(11), 15(18), 22(25)-tetrakis-(2-{2-[3(triethylamino)phenoxy]ethoxy}ethoxy) phthalocyaninato zinc(II) iodide (3)

Quaternized zinc(II) phthalocyanine **3** was prepared by our group according to the procedure given in the literature [34]. The procedure for the synthesis of (2-{2-[3-(diethylamino)phenoxy]ethoxy}ethoxy) group-substituted zinc(II) phthalocyanine (**2**) and its quaternized derivative (**3**) are illustrated in Fig. 1. Initially, (2-{2-[3-(diethylamino)phenoxy]ethoxy}ethoxy) group-substituted zinc(II) phthalocyanine **2** was prepared by cyclotetramerization of compound **1** in n-pentanol, DBU, and anhydrous $Zn(CH_3COO)_2$ at 160°C. Details of this procedure were already published by our group [34]. Quaternized zinc(II) phthalocyanine **3** was synthesized as per the following procedure: (2-{2-[3-(Diethylamino)phenoxy]ethoxy}ethoxy) group-substituted zinc(II) phthalocyanine (**2**) (0.050 g, 0.031 × 10⁻³ mol) was dissolved in 5 mL of chloroform, and 3.5 mL methyl iodide was added to this solution. The reaction mixture was stirred at room temperature (25°C) for 4 d. The green precipitate was filtered off, washed with chloroform, acetone, and diethyl ether. Finally, water-soluble quaternized zinc phthalocyanine **3** was dried in vacuum.

2.2. Preparation of the catalysts

All the reagents and solvents were purchased from Sigma. They were analytical grade and used without further purification.

Various nanoparticles were prepared in the presence and absence of ZnPc and/or TX100. The concentration of ZnPc was 1% of the mass of TiO_2. A modified sol–gel method was used for preparation of the all catalysts. The preparation procedures are given below.

An aliquot of 8.4 mL titanium (IV) isopropoxide (TiP) was dissolved in 20 mL absolute ethanol (solution A). Another portion of 10 mL absolute ethanol containing 1 mL concentrated HNO_3 and 1 mL of distilled water (solution B) was slowly added to solution A, and then, the mixture was left stirring for overnight. At the end of stirring, the mixture was dried at 80°C for 12 h. Finally, TiO_2 nanopowder was calcined for 4 h at 300°C and cooled down to room temperature. TiO_2 nanopowder was also prepared in the presence of surfactant and defined as TiO_2-TX100. Briefly, before adding TiP solution, a suitable amount of TX100 was homogeneously dissolved in absolute ethanol (solution A). Then, TiP solution was added during vigorous stirring. The molar ratio of the materials was at 1:5:1 (TiP: EtOH: TX100).

The $ZnPc/TiO_2$ composite containing 1% phthalocyanine was prepared as follows: Quaternized ZnPc (which is 1% of the mass of TiO_2) was dissolved in ethanol and added into solution A. Mixture was left stirring for 2 h. Then, solution B was slowly added into this solution, and the same drying/calcinations procedure was used to obtain $ZnPc/TiO_2$.

Finally, $ZnPc/TiO_2$-TX100 was prepared following the same procedure but adding TX100 into solution A before hydrolysis step.

2.3. Structural and surface analysis

A Rigaku D/Max-IIIC diffractometer with CuKα radiation (λ = 1.5406 Å) over the range 2θ = 20°–60° at room temperature was employed for XRD analysis of the catalysts. Specific surface area was measured using BET surface area analyzer (Micromeritics, ASAP 2020) using nitrogen as a purge gas, and pore volume (V_p) was estimated at P/P_o = 0.984 from the desorption batch. The surface morphology of the photocatalysts was examined using a SEM (SEM, ZEISS EVO LS-10, combined with EDX) and transmission electron microscope (TEM, FEI Tecnai G² spirit). Thermogravimetric analysis (TG/DTA, Seiko Exstar 6000) was performed to determine the structural variations under nitrogen atmosphere with a heating rate at 20°C/min between
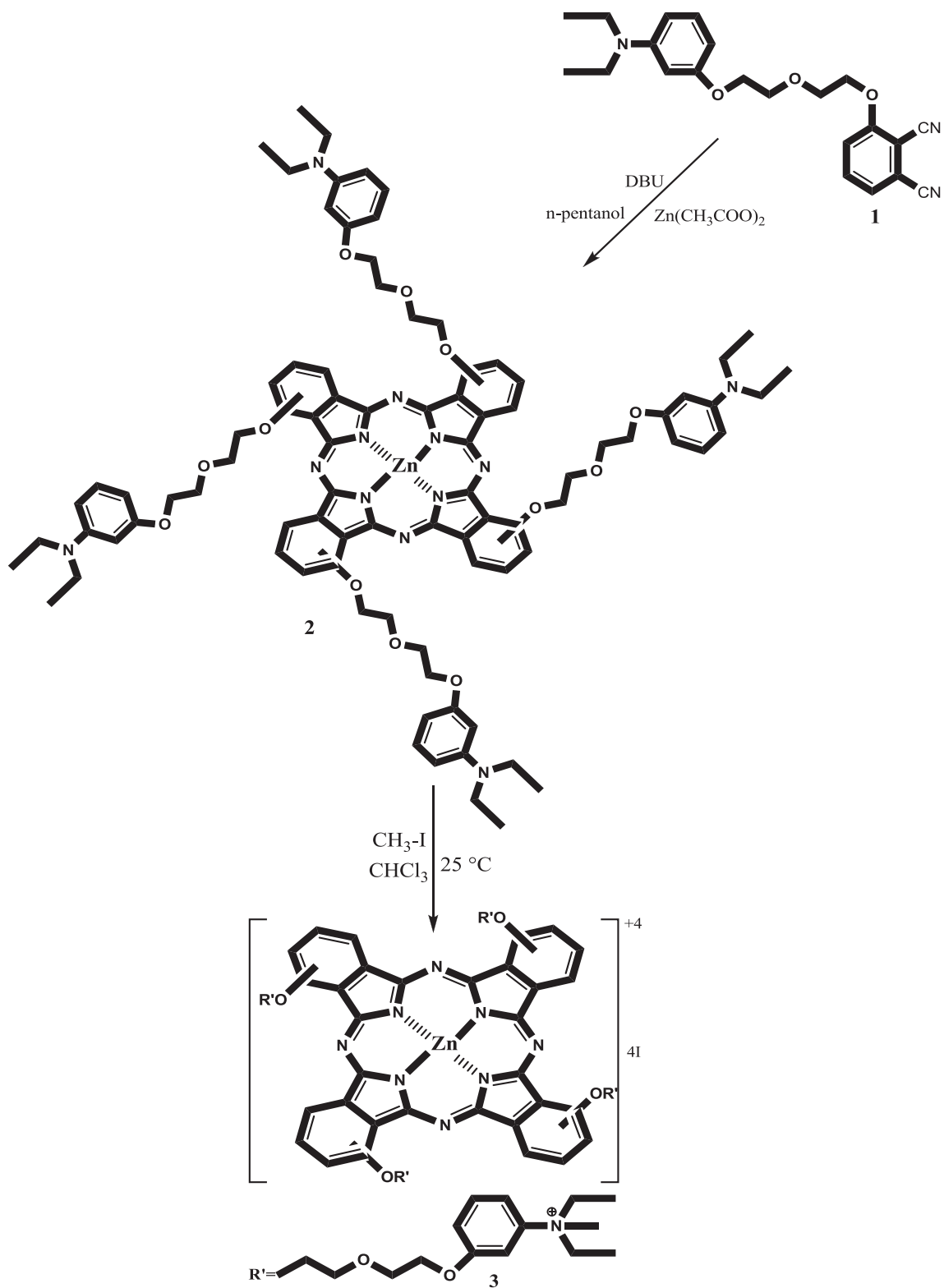
Fig. 1. The synthesis of quaternized zinc(II) phthalocyanine (3).

30 and 700°C temperature range in a platinum crucible. The UV–vis diffuse reflectance (DR) spectroscopy of the samples was recorded on Shimadzu UV-3600 UV–vis–NIR spectrophotometer.

2.4. Evaluation of photocatalytic activity

The photocatalytic efficiencies of the materials were evaluated by measuring the removal percentage of aqueous solution of methylene orange or Cr(VI) ions in the presence and absence of light. A set of experiments were designed to test the photocatalytic activity of the ZnPc-sensitized nanocomposite and compare with pure TiO_2. A 30 mL portion of aqueous solution of MO (10 mg L^{-1}) and 40 mg catalyst (1.33 g L^{-1}) were placed in a quartz cell. The lamp (2 × 8 W, 350 μW/cm^2, 365 nm) was positioned about 10 cm in front of the reaction cell. The reaction mixture was stirred continuously using a magnetic stirrer and sampled at regular time intervals and then centrifuged for 20 min at the rate of 4,000 rpm. Decrease in the concentrations of MO was monitored spectrophotometrically at $\lambda = 462$ nm (Unicam UV-2 spectrometer) in the presence and absence of light.

In the case of photo-reduction studies, 40 mg catalyst was suspended into 30 mL aqueous solutions containing $K_2Cr_2O_7$ solution (10 mg L^{-1} Cr(VI)), followed by adjusting pH to pH 2.0 with H_3PO_4 solution. The remaining Cr(VI) ions in the reaction mixture were determined over a certain treatment period using the diphenylcarbazide colorimetric method [35].

3. Results and discussion

3.1. Structural analysis of catalysts

TG-DTA technique was used to determine thermal behavior of ZnPc/TiO_2 nanocomposite (Fig. 2). TG-DTA curves of neat ZnPc (Fig. 2(a)) were also recorded to compare with ZnPc/TiO_2. The TG curves showed initial weight losses for ZnPc (25%) and ZnPc/TiO_2 nanocomposite (2%) from 25 to 150°C, which relates to endothermic peak in the DTA pattern can be ascribed to the desorption of the adsorbed water. Another weight loss for both the materials occurring at around 350°C was related with the exothermic peak in the DTA curve, which can be attributed to the combustion of the phthalocyanine molecule. The residual mass (88%) represents the mass of TiO_2 in ZnPc/TiO_2 nanocomposite (Fig. 2(b)). Therefore, the calcination temperature of the ZnPc/TiO_2 should not be higher than 300°C, which corresponds to the combustion temperature of ZnPc.

Fig. 3 presents the XRD pattern of the pure TiO_2 (a), TiO_2-TX100 (b), ZnPc/TiO_2 (c), and ZnPc/TiO_2-TX100 (d), respectively. The peaks of the ZnPc are not observed in XRD patterns of ZnPc/TiO_2 nanocomposite, which could be assigned to the non-crystalline of ZnPc [36]. In all samples, the patterns belonging to the anatase structure were observed, showing that the crystalline phase of TiO_2 has not changed through the ZnPc modification. After surface modification with TX100 or ZnPc, the crystalline size and peak ($2\theta = 25.24$) intensities of TiO_2 decreased compared to bare TiO_2 because of expansion of the line-width at half maximum of the X-ray diffraction peaks. The crystalline sizes of catalysts were determined by Scherrer's equation [37] using the line-width at half maximum of the X-ray diffraction peaks and shown in Table 1.

UV–vis DR spectra of samples are shown in Fig. 4. As can be seen from the figure, ZnPc/TiO_2 had broad absorption in 400–800 nm region. ZnPc-sensitized TiO_2 exhibited absorption bands in the wavelengths of 600–750 nm, which are corresponding to the Q bands of ZnPc. The optical absorption enhancement of the ZnPc/TiO_2 composite photocatalyst in visible region is attributed to Q band absorption and resulted from $\pi \rightarrow \pi^*$ transition of the molecular orbital of the respective phthalocyanine. However, TiO_2 showed only absorption in the UV region and had no more absorption in visible region beyond 400 nm [38,39]. Consequently, ZnPc/TiO_2 photocatalyst could extend the absorption spectrum of TiO_2 into visible region, and it could possibly exhibit better photocatalytic activity.

The surface areas of the prepared catalysts (TiO_2, TiO_2-TX100, ZnPc/TiO_2, and ZnPc/TiO_2-TX100) were measured by nitrogen adsorption at −196.24°C. The surface area (S_{BET} (m^2 g^{-1})) was calculated and found to be 16.204, 23.994, 110.045, and 343.267 m^2 g^{-1}, and the pore volume of the samples (Fig. S in the Supplementary Information) was also determined to be 0.017, 0.024, 0.011, and 0.056 cm^3 g^{-1} for TiO_2, TiO_2-TX100, ZnPc/TiO_2, and ZnPc/TiO_2-TX100, respectively (Table 1). The catalysts with a higher pore volume and surface area can absorb more O_2 from air, resulting in the deceleration of excited electrons transfer from TiO_2 to Pc$^{·+}$ and enhancement of the removal of MO by Pc$^{·+}$.

The SEM mapping images (Fig. 5) confirm that ZnPc molecule are attached well on the surface of the TiO_2 photocatalyst because of Zn atoms, which are located in the center of the ZnPc, are uniformly distributed on the ZnPc/TiO_2 nano composite. Fig. 6 shows the EDX spectra of the samples. The EDX analyses could also confirm that the ZnPc was
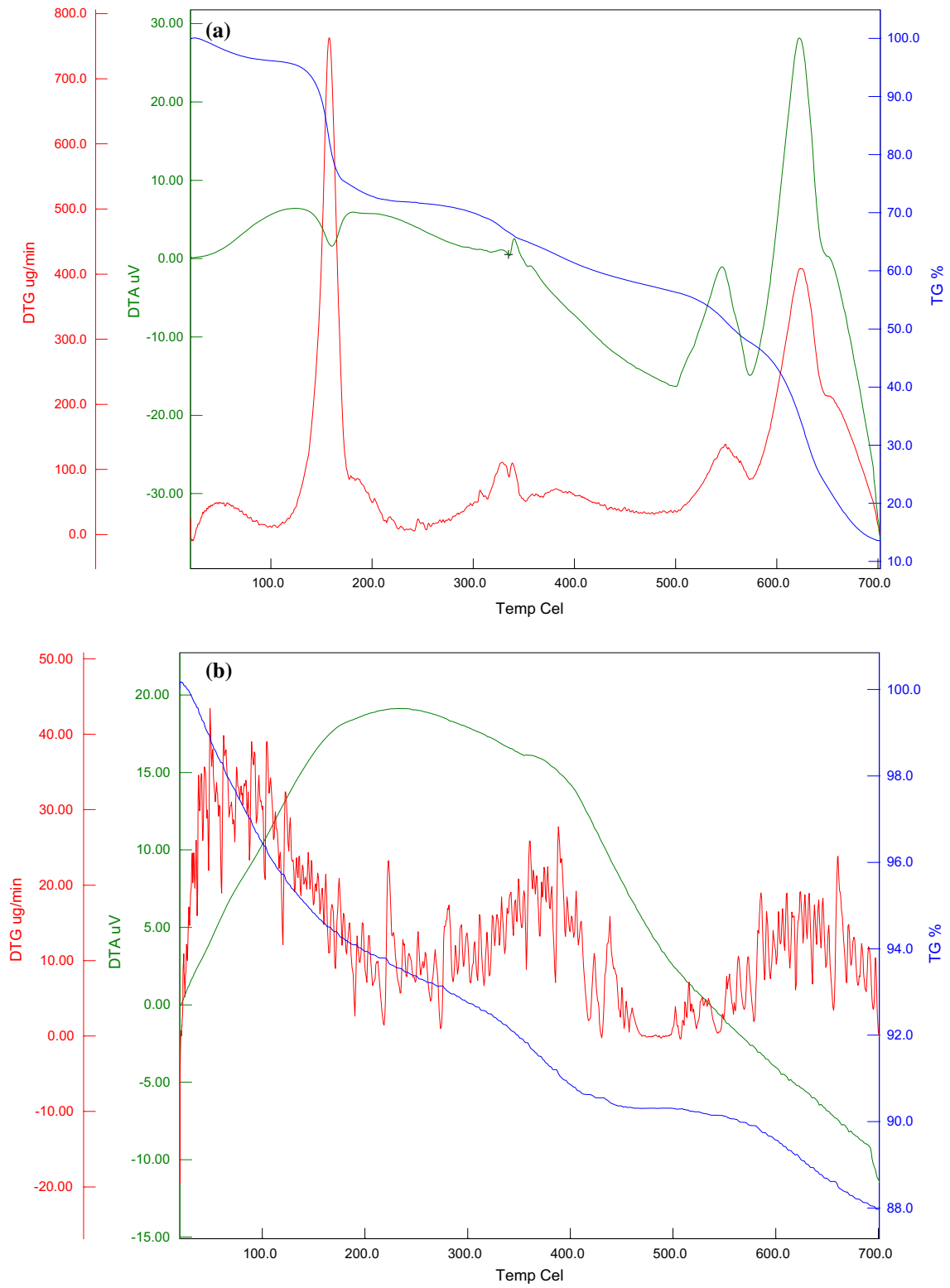
Fig. 2. TG-DTA curves of the ZnPc (a) and ZnPc/TiO$_2$ nanocomposite (b).
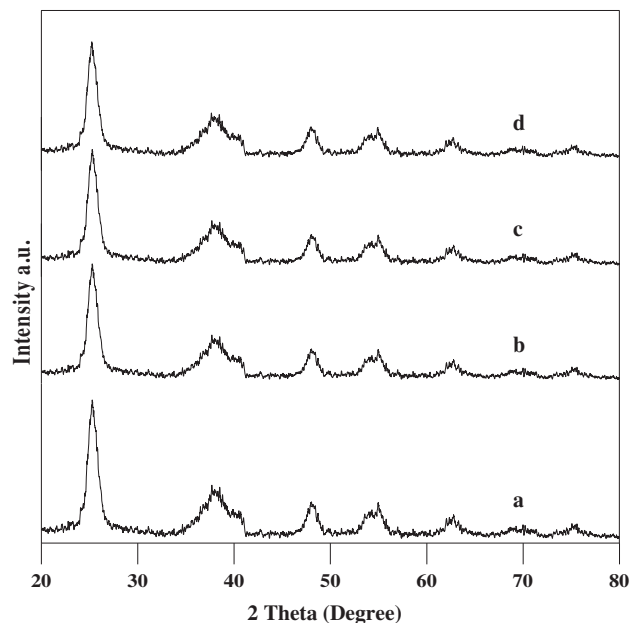
Fig. 3. XRD patterns for pure TiO_2 (curve a), TiO_2-TX100 (curve b), $ZnPc/TiO_2$ (curve c), and $ZnPc/TiO_2$-TX100 (curve d).
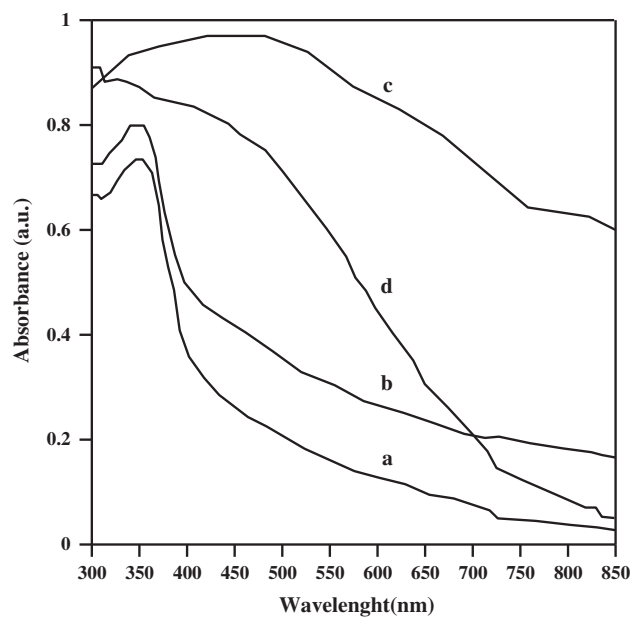
Fig. 4. UV–visible spectra of pure TiO_2 (a), TiO_2-TX100 (b), $ZnPc/TiO_2$ (c), and $ZnPc/TiO_2$-TX100 (d).

Table 1
Structural characteristics of TiO_2 particles

Catalysts	S_{BET} ($m^2\ g^{-1}$)	[a]PS, pore size (nm)	[b]V_{pore} ($cm^3\ g^{-1}$)	[c]CS, crystalline size (nm)
TiO_2	16.204	3.255	0.017	18.72
TiO_2-TX 100	23.994	3.103	0.024	13.29
$ZnPc/TiO_2$	110.045	2.762	0.011	12.09
$ZnPc/TiO_2$-TX 100	343.267	2.296	0.056	10.14

[a]Average pore diameter calculated from BJH desorption average pore width (4 V/A).
[b]Single point total pore volume at the relative pressure of ca. 0.966.
[c]Calculated by the Scherrer's equation.

successfully doped in the TiO_2 nanoparticles successfully due to the presence of zinc, oxygen, nitrogen, and titanium signals.

The morphology of $ZnPc/TiO_2$ was observed by TEM (Fig. 7). The synthesized nanoparticles have spherical-like structures, favoring increased photocatalytic activity. Also, we can note that there is an extensive agglomeration because ZnPc had covered TiO_2 superficially. $ZnPc/TiO_2$ nanoparticles have an average crystalline grain diameter about 5–15 nm, which was in agreement with the XRD results. Since the substituted groups on ZnPc are not located at axial position, it tends to aggregation. Therefore, it is not clear which phase is TiO_2 or ZnPc from the TEM image. However, lighter area is considered as organic phase (ZnPc) and darker spots on organic phase is inorganic TiO_2.

3.2. Photocatalytic experiments

The photocatalytic activities of ZnPc-sensitized TiO_2 samples were investigated in terms of the removal of the MO or Cr(VI) ions in aqueous suspensions under near visible light irradiation. The photocatalytic removal experiments were repeated in the presence and absence of light and catalyst. The efficiency of the removal of pollutants was defined as C/C_o, where C_o and C are concentrations of the pollutants at initial and a given reaction time (min), respectively. According to the data given in Fig. 8, MO was highly resistant to degradation and a slight decomposition was observed in the absence of photocatalyst. As can be seen from Fig. 8(a), the degradation ratio of MO using $ZnPc/TiO_2$ composite was 43.9% which
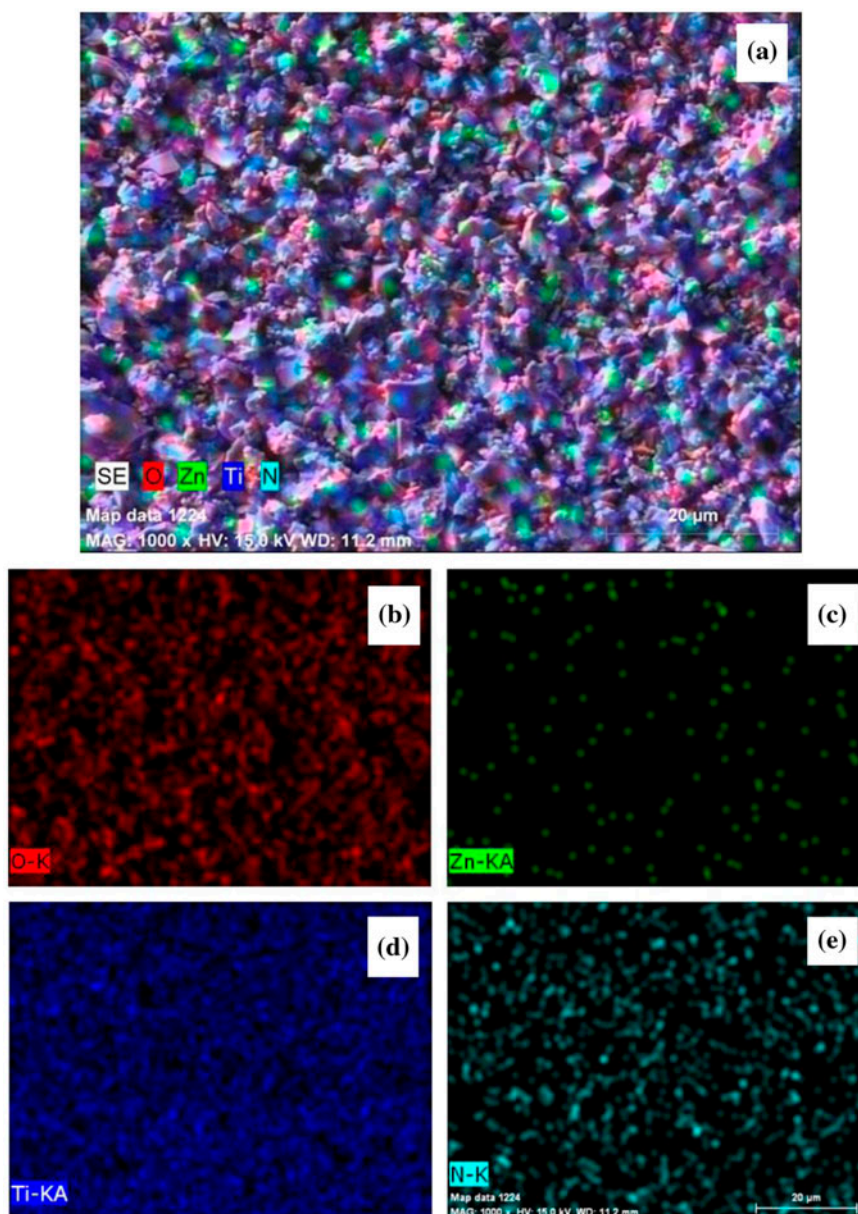
Fig. 5. SEM mapping image of ZnPc/TiO$_2$ nanocomposite: Elemental distribution of ZnPc/TiO$_2$ nanocomposite (a), O (b), Zn (c), Ti (d), and N (e) mapping images of the nanocomposite.

was much higher than pure TiO$_2$ (24.05%) after 150 min irradiation. In particular, degradation ratios using the ZnPc/TiO$_2$-TX100 and TiO$_2$-TX100 composites reached to 57.60 and 36.84%, respectively, which showed an increase as compared to the catalyst prepared without surfactant. After 150 min of irradiation, the photocatalytic activity of the prepared catalysts using sol–gel or sol–gel modified with TX100 follows the order ZnPc/TiO$_2$-TX100 > ZnPc/TiO$_2$ > TiO$_2$-TX100 > TiO$_2$. It was found that there was no significant degradation in the presence or absence of the prepared photocatalyst in dark experiments (Fig. 8(b)). Our results showed that the presence of sensitizer and using surfactant during catalyst preparation play an important role in the photocatalytic activity of TiO$_2$.

In addition, the photocatalytic reduction of Cr(VI) to Cr(III) was also investigated. To test the photocatalytic reduction ability of the catalysts, Cr(VI) ions were chosen as the target toxic pollutant. Fig. 9 shows the relationship between C/C_o ratio and irradiation
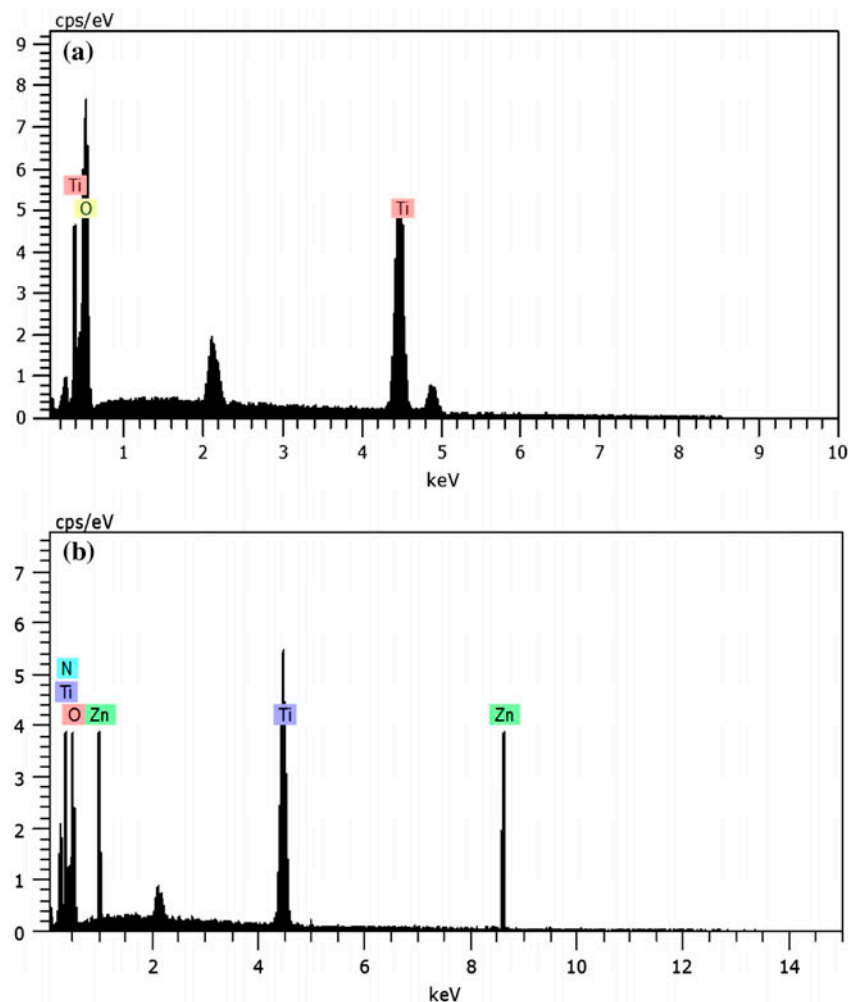
Fig. 6. EDX spectra of TiO_2-TX100 (a) and ZnPc/TiO_2-TX100 (b).

time. The formation of Cr(III) is much more effective for ZnPc/TiO_2-TX100 catalyst (100%) than pure TiO_2 (60%) after 150 min irradiation. The photocatalytic reduction activity order of the catalysts is as follows:

ZnPc/TiO_2-TX100 > ZnPc/TiO_2 > TiO_2-TX100 > TiO_2.
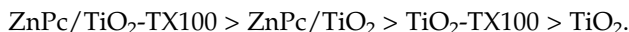
The photochemical reduction of Cr(VI) was negligible when the Cr(VI) solution was not irradiated with UV light (Fig. 9(a)). Triplicate runs were carried out for each test (for the removal of MO or Cr(VI) ions), and the relative standard deviations were calculated for each treatment and generally less than 1%.

It should be noted that the removal in the dark experiments are simple adsorption rather than reduction. The removal results showed that the removal ratio of the test pollutants (MO or Cr(VI) ions) over the ZnPc/TiO_2-TX100 catalyst, which was synthesized using sol–gel modified with TX100, is the highest one especially Cr(VI) photocatalytic reduction in near visible light irradiation. The results can be attributed to the below reasons:

(1) The phthalocyanine in the solid state is a p-type semiconductor characterized by energy of the band gap about 2.0 eV [40,41]. So, the phthalocyanine-sensitized TiO_2 photocatalyst can be excited by visible light irradiation to produce photo-excited electrons (e^-) and positive holes (h^+) and the transfer to TiO_2 and ZnPc, respectively. Then, excited phthalocyanine can generate $^1O_2$ and $Pc^{·+}$ to degrade MO. At the same time, the photo-excited electrons transfer to CB of TiO_2 and the photocatalytic reduction of Cr(VI) to Cr(III) is carried out by these trapped electrons.
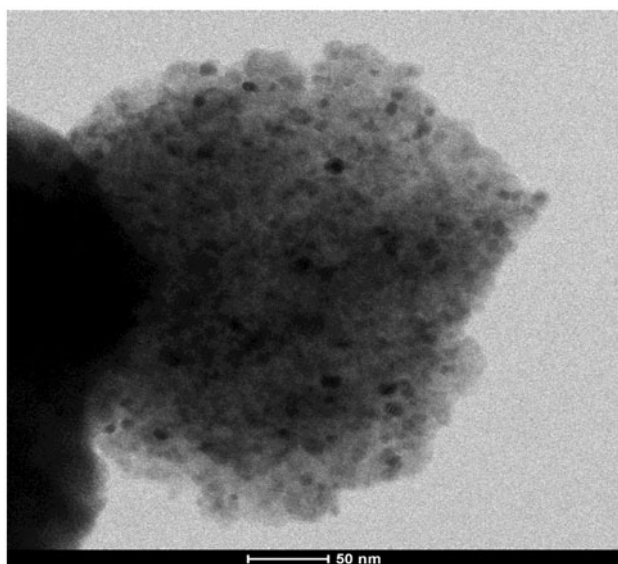
Fig. 7. The TEM image of the ZnPc/TiO$_2$ nanocomposite.
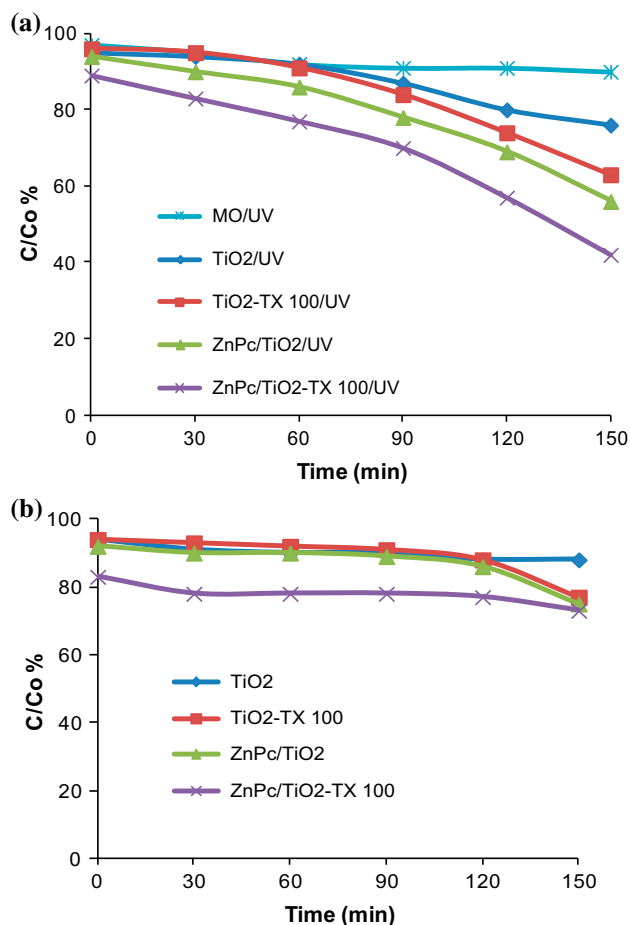
Fig. 8. The removal of MO with near visible light irradiation (a) and the removal of MO in the dark in the presence of the catalysts (b).
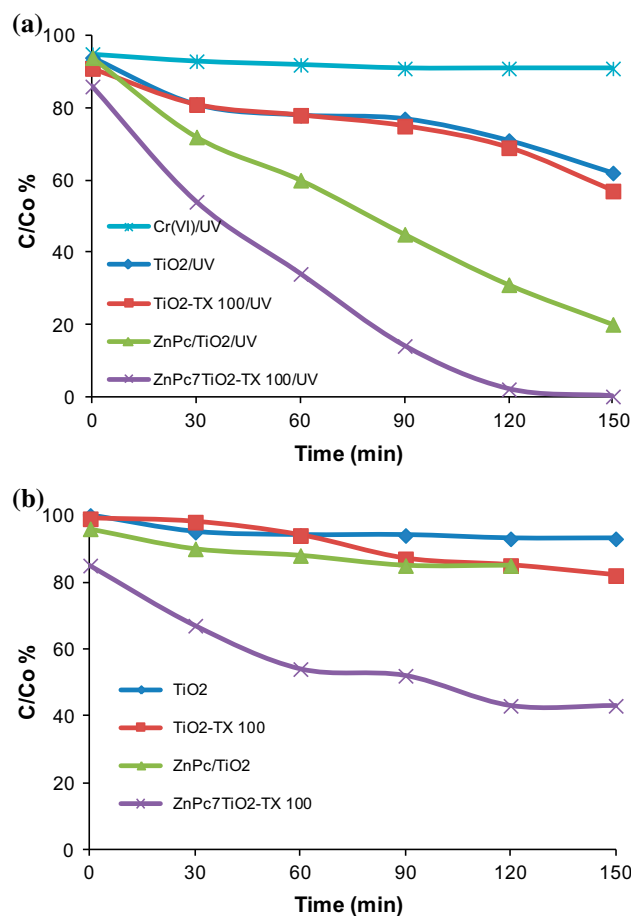
Fig. 9. The photocatalytic reduction of Cr(VI) with near visible light irradiation (a) and the removal of Cr(VI) in the dark in the presence of the catalysts (b).

(2) ZnPc/TiO$_2$ inhibits the recombination of holes and electrons because Pc rapidly transfers photo-excited electrons to the conduction of TiO$_2$. Therefore, the photocatalytic activity can be significantly improved [42]. It should be noted that quaternized groups attached to ZnPc have some important features. First of all, this substituted long chain increases the polarity of ZnPc resulting in a better attachment to TiO$_2$ surface. As a result, electron transfer from ZnPc to TiO$_2$ is more possible. Secondly, quaternized N atoms are more likely to absorb the photons and readily excited to ZnPc*. As a combination of all these factors, electron transfer is enhanced and so do photocatalytic action.

(3) Another reason is that ZnPc/TiO$_2$-TX100 with high surface area and pore volume can absorb much oxygen on the inside or outside to form reactive and effective oxygen species. Thus, ZnPc/TiO$_2$-TX100 composite may lead to faster

removal of pollutants. The same tendency was observed for both ZnPc/TiO$_2$-TX100 and TiO$_2$-TX100 catalysts that were prepared in the presence of TX100. This is a good evidence of how particle size and surface area effect the catalytic action of heterogeneous catalysis.

Based on these possibilities, transfer of excited electrons enhances the recombination and adsorption capacity, and ZnPc/TiO$_2$-TX100 could well improve the photocatalytic activity.

4. Conclusions

In this study, anatase nano-sized TiO$_2$ particles and ZnPc/TiO$_2$ nanocomposite were successfully synthesized by sol–gel method. The prepared catalysts especially ZnPc/TiO$_2$ had enhanced structural and photocatalytic properties including high surface area and pore volume using sol–gel modified with TX100 surfactant. The morphology of ZnPc/TiO$_2$ was characterized using SEM, EDX, XRD, TGA, BET, TEM, and UV–vis–NIR. The results of morphological analysis revealed that the ZnPc/TiO$_2$-TX100 nanocomposite has higher surface area and pore volume than other catalysts (ZnPc, TiO$_2$-TX100, and TiO$_2$). ZnPc caused a significant absorption shift into the visible region. However, it did not change the crystal phase of TiO$_2$. Among the catalysts studied, ZnPc/TiO$_2$-TX100 composite presented the best photocatalytic activity, followed by ZnPc/TiO$_2$, TiO$_2$-TX100 and TiO$_2$ for the removal of both Cr(VI) and MO in water. Above all, the prepared composite employing TX100 surfactant is a promising photocatalyst for environmental applications.

Supplementary materials

The supplementary material for this paper is available online at http://dx.doi.10.1080/19443994.2015.1084535.

Acknowledgements

References

[1] T. Ohno, K. Tokieda, S. Higashida, M. Matsumura, Synergism between rutile and anatase TiO$_2$ particles in photocatalytic oxidation of naphthalene, Appl. Catal., B: Environ. 244 (2003) 383–391.

[2] F.M.D. Oliveira, P.S. Batista, P.S. Muller Jr., V. Velani, M.D. França, D.R. de Souza, A.E.H. Machado, Evaluating the effectiveness of photocatalysts based on titanium dioxide in the degradation of the dye Ponceau 4R, Dyes Pigm. 92 (2011) 563–572.

[3] T. Jiang, L. Zhang, M. Ji, Q. Wang, Q. Zhao, X. Fu, H. Yin, Carbon nanotubes/TiO$_2$ nanotubes composite photocatalysts for efficient degradation of methyl orange dye, Particuology 11 (2013) 737–742.

[4] N. Panda, H. Sahoo, S. Mohapatra, Decolourization of methyl orange using Fenton-like mesoporous Fe$_2$O$_3$–SiO$_2$ composite, J. Hazard. Mater. 185 (2011) 359–365.

[5] M.A. Behnajady, N. Mansoriieh, N. Modirshahla, M. Shokri, Influence of operational parameters and kinetics analysis on the photocatalytic reduction of Cr (VI) by immobilized ZnO, Environ. Technol. 33 (2012) 265–271.

[6] J.F. Blais, S. Shen, N. Meunier, R.D. Tyagi, Comparison of natural adsorbents for metal removal from acidic effluent, Environ. Technol. 24 (2003) 205–215.

[7] C. Chen, W. Ma, J. Zhao, Semiconductor-mediated photodegradation of pollutants under visible-light irradiation, Chem. Soc. Rev. 39 (2010) 4206–4219.

[8] Y. Jiang, L. Guo, W. Zhang, F. Dai, Y. Yan, F. Zhang, H. Lv, Preparation of zinc tetraaminophthalocyanine sensitized TiO$_2$ hollow nanospheres and their enhanced photocatalytic properties under visible light, Desalin. Water Treat. 52 (2014) 3489–3496.

[9] G. Mele, R. Del Sole, G. Vasapollo, E. García-López, L. Palmisano, M. Schiavello, Photocatalytic degradation of 4-nitrophenol in aqueous suspension by using polycrystalline TiO$_2$ impregnated with functionalized Cu (II)–porphyrin or Cu(II)-phthalocyanine, J. Catal. 217 (2003) 334–342.

[10] N. Yazdanpour, S. Sharifnia, Photocatalytic conversion of green house gases (CO$_2$ and CH$_4$) using copper phthalocyanine modified TiO$_2$, Sol. Energy Mater. Sol. Cells 118 (2013) 1–8.

[11] L.F. Cueto, G.A. Hirata, E.M. Sánchez, Thin-film TiO$_2$ electrode surface characterization upon CO$_2$ reduction processes, J. Sol-Gel Sci. Technol. 37 (2006) 105–109.

[12] G. Palmisano, V. Augugliaro, M. Pagliaro, L. Palmisano, Photocatalysis: A promising route for 21st century organic chemistry, Chem. Commun. 33 (2007) 3425.

[13] M.N. Chong, B. Jin, C.W.K. Chow, C. Saint, Recent developments in photocatalytic water treatment technology: A review, Water Res. 44 (2010) 2997–3027.

[14] M.R. Hoffman, S.T. Martin, W. Choi, D.W. Bahnemann, Environmental applications of semiconductor photocatalysis, Chem. Rev. 95 (1995) 95–96.

[15] S. Banerjee, S.C. Pillai, P. Falaras, K.E. O'Shea, J.A. Byrne, D.D. Dionysiou, New insights into the mechanism of visible light photocatalysis, J. Phys. Chem. Lett. 5 (2014) 2543–2554.

[16] A. Khalil, M.A. Gondal, M.A. Dastageer, Augmented photocatalytic activity of palladium incorporated ZnO nanoparticles in the disinfection of Escherichia coli microorganism from water, Appl. Catal., A: Gen. 402 (2011) 162–167.

[17] N. Wang, Y. Xu, L. Zhu, X. Shen, H. Tang, Reconsideration to the dectivation of TiO$_2$ catalyst during simultaneous photocatalytic reduction of Cr(VI) and oxidation of salicylic acid, J. Photochem. Photobiol., A: Chem. 201 (2009) 121–127.

[18] T.T. Isimjan, H. Kazemian, S. Rohani, A.K. Ray, Photocatalytic activities of Pt/ZIF-8 loaded highly ordered TiO_2 nanotubes, J. Mater. Chem. 20 (2010) 10241–10245.

[19] P. Huo, Y. Yan, S. Li, H. Li, W. Huang, Preparation and characterization of Cobalt Sulfophthalocyanine/TiO_2/fly-ash cenospheres photocatalyst and study on degradation activity under visible light, Appl. Surf. Sci. 255 (2009) 6914–6917.

[20] V.C. Papadimitriou, V.G. Stefanopoulos, M.N. Romanias, P. Papagiannakopoulos, K. Sambani, V. Tudose, G. Kiriakidis, Determination of photo-catalytic activity of un-doped and Mn-doped TiO_2 anatase powders on acetaldehyde under UV and visible light, Thin Solid Films 520 (2011) 1195–1201.

[21] H.G. Yu, H. Irie, Y. Shimodaira, Y. Hosogi, Y. Kuroda, M. Miyauchi, K. Hashimoto, An efficient visible-light-sensitive Fe(III)-grafted TiO_2 photocatalyst, J. Phys. Chem. C 114 (2010) 16481–16487.

[22] J. Wang, Z.Q. Lin, Dye-sensitized TiO_2 nanotube solar cells with markedly enhanced performance via rational surface engineering, Chem. Mater. 22 (2010) 579–584.

[23] J.S. Jang, H.G. Kim, U.A. Joshi, J.W. Jang, J.S. Lee, Fabrication of CdS nanowires decorated with TiO_2 nanoparticles for photocatalytic hydrogen production under visible light irradiation, Int. J. Hydrogen Energy 33 (2008) 5975–5980.

[24] Q. Sun, Y. Xu, Sensitization of TiO_2 with aluminum phthalocyanine: Factors influencing the efficiency for chlorophenol degradation in water under visible light, J. Phys. Chem. C 113 (2009) 12387–12394.

[25] Z. Wang, W. Mao, H. Chen, F. Zhang, X. Fan, G. Qian, Copper(II) phthalocyanine tetrasulfonate sensitized nanocrystalline titania photocatalyst: Synthesis *in situ* and photocatalysis under visible light, Catal. Commun. 7 (2006) 518–522.

[26] H. Xu, F. Wu, M. Li, Z. Liang, Application of response surface methodology for optimization of nano-TiO_2 preparation using modified sol-gel method, J. Sol-Gel Sci. Technol. 67 (2013) 394–405.

[27] H. Choi, E. Stathatos, D.D. Dionysiou, Synthesis of nanocrystalline photocatalytic TiO_2 thin films and particles using sol-gel method modified with nonionic surfactants, Thin Solid Films 510 (2006) 107–114.

[28] R. Xing, L. Wu, Z. Fei, P. Wu, Palladium phthalocyaninesulfonate functionalized mesoporous polymer: A highly efficient photocatalyst for degradation of 4-chlorophenol under visible light irradiation, J. Mol. Catal. A: Chem. 371 (2013) 15–20.

[29] A. Sun, Z. Xiong, Y. Xu, Removal of malodorous organic sulfides with molecular oxygen and visible light over metal phthalocyanine, J. Hazard. Mater. 152 (2008) 191–195.

[30] M. Hu, Y. Xu, J. Zhao, Efficient photosensitized degradation of 4-chlorophenol over immobilized aluminum tetrasulfophthalocyanine in the presence of hydrogen peroxide, Langmuir 20 (2004) 6302–6307.

[31] S.-H. Wu, J.-L. Wu, S.-Y. Jia, Q.-W. Chang, H.-T. Ren, Y. Liu, Cobalt(II) phthalocyanine-sensitized hollow Fe_3O_4@SiO_2@TiO_2 hierarchical nanostructures: Fabrication and enhanced photocatalytic properties, Appl. Surf. Sci. 287 (2013) 389–396.

[32] Z. Guo, B. Chen, J. Mu, M. Zhang, P. Zhang, Z. Zhang, J. Wang, X. Zhang, Y. Sun, C. Shao, Y. Liu, Iron phthalocyanine/TiO_2 nanofiber heterostructures with enhanced visible photocatalytic activity assisted with H_2O_2, J. Hazard. Mater. 219–220 (2012) 156–163.

[33] Q. Wang, W. Wu, J. Chen, G. Chu, K. Ma, H. Zou, Novel synthesis of ZnPc/TiO_2 composite particles and carbon dioxide photo-catalytic reduction efficiency study under simulated solar radiation conditions, Colloids Surf., A: Physicochem. Eng. Aspects 409 (2012) 118–125.

[34] V. Çakır, D. Çakır, M. Göksel, M. Durmuş, Z. Bıyıklıoğlu, H. Kantekin, Synthesis, photochemical, bovine serum albumin and DNA binding properties of tetrasubstituted zinc phthalocyanines and their water soluble derivatives, J. Photochem. Photobiol., A: Chem. 299 (2015) 138–151.

[35] M.V. Dozzi, A. Saccomanni, E. Selli, Cr(VI) photocatalytic reduction: Effects of simultaneous organics oxidation and of gold nanoparticles photodeposition on TiO_2, J. Hazard. Mater. 211–212 (2012) 188–195.

[36] K. Vignesh, M. Rajarajan, A. Suganthi, Photocatalytic degradation of erythromycin under visible light by zinc phthalocyanine-modified titania nanoparticles, Mater. Sci. Semicond. Process. 23 (2014) 98–103.

[37] W. Mekprasart, N. Vittayakorn, W. Pecharapa, Ball-milled CuPc/TiO_2 hybrid nanocomposite and its photocatalytic degradation of aqueous Rhodamine B, Mater. Res. Bull. 47 (2012) 3114–3119.

[38] Z.C. Guo, B. Chen, M.Y. Zhang, J.B. Mu, C. Shao, Y.C. Liu, Zinc phthalocyanine hierarchical nanostructure with hollow interior space: Solvent–thermal synthesis and high visible photocatalytic property, J. Colloid Interface Sci. 348(1) (2010) 37–42.

[39] Z.D. Popovic, A study of carrier generation in β-metal-free phthalocyanine, Chem. Phys. 86 (1984) 311–321.

[40] V. Iliev, Phthalocyanine-modified titania-catalyst for photooxidation of phenols by irradiation with visible light, J. Photochem. Photobiol., A Chem. 151 (2002) 195–199.

[41] N. Bao, Y. Li, Z. Wei, G. Yin, J. Niu, Adsorption of dyes on hierarchical mesoporous TiO_2 fibers and its enhanced photocatalytic properties, J. Phys. Chem. C 115 (2011) 5708–5719.

[42] Z. Mesgari, M. Gharagozlou, A. Khosravi, K. Gharanjig, Synthesis, characterization and evaluation of efficiency of new hybrid Pc/Fe-TiO_2 nanocomposite as photocatalyst for decolorization of methyl orange using visible light irradiation, Appl. Catal., A: Gen. 411–412 (2012) 139–145.